

## Original articles

Research article

<https://doi.org/10.17308/kcmf.2025.27/13322>

### Phase equilibria in the GeTe-Sb<sub>2</sub>Te<sub>3</sub>-Te system

E. R. Nabiiev<sup>1</sup>, E. N. Orujlu<sup>2</sup>✉, A. A. Hasanov<sup>2</sup>, A. I. Aghazade<sup>3</sup>, S. H. Aliyeva<sup>4</sup>, Yu. A. Yusibov<sup>1</sup>

<sup>1</sup>Ganja State University,  
429 H. Aliyev ave., Ganja AZ-2001, Azerbaijan

<sup>2</sup>Azerbaijan State Oil and Industry University,  
16/21 Azadliq ave., Baku AZ-1010, Azerbaijan

<sup>3</sup>Institute of Catalysis and Inorganic Chemistry,  
113 H. Javid ave., Baku AZ-1143, Azerbaijan

<sup>4</sup>Nakhchivan State University,  
1 H. Aliyev ave., Nakhchivan AZ-7000, Azerbaijan

#### Abstract

**Objectives:** Germanium-antimony tellurides are of considerable practical interest as thermoelectrics with low thermal conductivity, topological insulators and phase memory materials. In this paper, the results of a study of phase equilibria in the region of GeTe-Sb<sub>2</sub>Te<sub>3</sub>-Te compositions of the Ge-Sb-Te system using the DTA, X-ray diffraction and SEM methods are presented.

**Experimental:** The studied samples were synthesized using a special technique that allows them to be obtained in a state as close to equilibrium as possible.

**Conclusions:** A diagram of solid-phase equilibria at 300 K, a projection of the liquidus surface and some polythermal sections of the phase diagram are constructed. The fields of primary crystallization of phases are outlined, non- and monovariant equilibria are determined. According to the obtained picture of phase equilibria, the curves of monovariant equilibria originating from the peritectic and eutectic points of the boundary system GeTe-Sb<sub>2</sub>Te<sub>3</sub> undergo transformations at certain transition points. In the region of compositions rich in tellurium, a number of invariant transition reactions occur, corresponding to the joint crystallization of two-phase mixtures of telluride phases and elemental tellurium.

**Keywords:** Layered germanium-antimony tellurides, Phase memory materials, Topological insulator, Phase diagram

**Funding:** The work was partially supported by the Azerbaijan Science Foundation - Grant No AEF-MCG-2022-1(42)-12/10/4-M-10.

**For citation:** Nabiiev E. R., Orujlu E. N., Hasanov A. A., Aghazade A. I., Aliyeva S. G., Yusibov Yu. A. Phase equilibria in the GeTe-Sb<sub>2</sub>Te<sub>3</sub>-Te system. *Condensed Matter and Interphases*. 2024;26(4): 639–650. <https://doi.org/10.17308/kcmf.2025.27/13322>

**Для цитирования:** Набиев Э. Р., Оруджлу Э. Н., Гасанов А. А., Агазаде А. И., Алиева С. Г., Юсубов Ю. А. Фазовые равновесия в системе GeTe-Sb<sub>2</sub>Te<sub>3</sub>-Te. *Конденсированные среды и межфазные границы*. 2025;26(4), 639–650. <https://doi.org/10.17308/kcmf.2025.27/13322>

✉ Elnur N. Orujlu, e-mail: elnur.oruclu@yahoo.com

© Nabiiev E. R., Orujlu E. N., Hasanov A. A., Aghazade A. I., Aliyeva S. G., Yusibov Yu. A., 2025



The content is available under Creative Commons Attribution 4.0 License.

## 1. Introduction

Ternary compounds of the A<sup>IV</sup>-B<sup>V</sup>-Te systems (A<sup>IV</sup>-Ge, Sn, Pb; B<sup>V</sup>-Sb, Bi) with layered tetradymite-like structures have long been in the focus of researchers as thermoelectric materials with anomalously low thermal conductivity [1-6]. The discovery at the beginning of our century of a new quantum state of matter - a topological insulator [7, 8] gave a new powerful impetus to the study of these compounds and phases based on them. It turned out that compounds of the homologous series A<sup>IV</sup>Te·mB<sup>V</sup><sub>2</sub>Te<sub>3</sub> (A<sup>IV</sup>B<sup>V</sup><sub>2</sub>Te<sub>4</sub>, A<sup>IV</sup>B<sup>V</sup><sub>4</sub>Te<sub>7</sub>, A<sup>IV</sup>B<sup>V</sup><sub>6</sub>Te<sub>10</sub>, etc.) and solid solutions based on them are 3D topological insulators and are very promising for use in various areas of high technology, including spintronics, quantum computers, scanning devices used in security systems and medicine, etc. [9-17].

Recently, the special attention of researchers has been attracted by compounds and alloys of the GeTe-Sb<sub>2</sub>Te<sub>3</sub> system with a reversible phase transition between the crystalline and amorphous states caused by very short (only a few tens of nanoseconds) laser radiation. These alloys, called phase memory materials, are already used as memory materials in rewritable optical disks and have great potential for creating a non-volatile alternative based on them to traditional flash memory [18-24].

At the initial of research stage on the development of new complex inorganic materials, particularly chalcogenide materials, it is essential to have reliable data on phase equilibria in the corresponding systems [25-29]. In the review article [26], based on a critical analysis of the available literature, it was shown that the data on the phase diagrams of most A<sup>IV</sup>Te-B<sup>V</sup><sub>2</sub>Te<sub>3</sub> type systems are contradictory and need to be clarified. Taking this into account, we have undertaken repeated detailed studies of phase equilibria in some A<sup>IV</sup>Te-B<sup>V</sup><sub>2</sub>Te<sub>3</sub> type systems using a specially developed technique for synthesizing equilibrium samples, as well as the thermodynamic properties of intermediate phases [30-37].

Numerous works [38-46] are devoted to the study of phase equilibria in the Ge-Sb-Te system, some of which are summarized in [43]. According to the data of [38], in the GeTe-Sb<sub>2</sub>Te<sub>3</sub> quasi-binary system, ternary compounds Ge<sub>2</sub>Sb<sub>2</sub>Te<sub>5</sub>, GeSb<sub>2</sub>Te<sub>4</sub>, GeSb<sub>4</sub>Te<sub>7</sub> are formed, melting with

decomposition according to peritectic reactions at 903, 888, and 875 K, respectively, as well as wide regions of solid solutions based on both initial compounds. The results of the study of phase equilibria in the GeTe-Sb<sub>2</sub>Te<sub>3</sub>-Te compositions region are presented in [39], and in [40, 41] in the Ge-GeTe-Sb<sub>2</sub>Te<sub>3</sub>-Sb compositions region. The results of the thermodynamic study of some ternary compounds of the GeTe-Sb<sub>2</sub>Te<sub>3</sub> system by the calorimetric method are presented in [42].

The papers [44, 45], published at the beginning of our century, present the results of repeated studies of solid-phase equilibria in the Ge-Sb-Te system and crystal structures of germanium-antimony tellurides. The authors of [44] presented a compilation phase diagram of the GeTe-Sb<sub>2</sub>Te<sub>3</sub> system, constructed based on the data of [38] with the addition of compositions of other known and suspected ternary compounds without specifying the nature and temperatures of their melting (Fig. 1a). Taking into account the compilation nature of this diagram, a new detailed study of this system was undertaken in [46]. It was shown that it is characterized by the presence of six ternary compounds: Ge<sub>4</sub>Sb<sub>2</sub>Te<sub>7</sub>, Ge<sub>3</sub>Sb<sub>2</sub>Te<sub>6</sub>, Ge<sub>2</sub>Sb<sub>2</sub>Te<sub>5</sub>, GeSb<sub>2</sub>Te<sub>4</sub>, GeSb<sub>4</sub>Te<sub>7</sub>, and GeSb<sub>6</sub>Te<sub>10</sub>. The first two melt with decomposition by a solid-phase reaction, and the rest - by peritectic reactions at 863, 854, 848, and 843 K, respectively (Fig. 1). In addition, in [46] the refined parameters of the crystal lattices of all the indicated compounds are presented.

New data obtained in [46] for the key section GeTe-Sb<sub>2</sub>Te<sub>3</sub> of the ternary system Ge-Sb-Te indicate the need to revise its complete T-x-y diagram and determine the primary crystallization fields of all identified ternary compounds.

Taking into account the above, we have undertaken a re-examination of phase equilibria in the Ge-Sb-Te system. In this paper, a new refined picture of phase equilibria of the indicated system in the GeTe-Sb<sub>2</sub>Te<sub>3</sub>-Te compositions range is presented, including the liquidus surface projection, the isothermal section at 300 K, and some polythermal sections of the phase diagram.

## 2. Experimental

### 2.1. Synthesis

The alloys for the study were prepared in 2 stages. At the first stage, the initial binary tellurides GeTe and Sb<sub>2</sub>Te<sub>3</sub> were synthesized

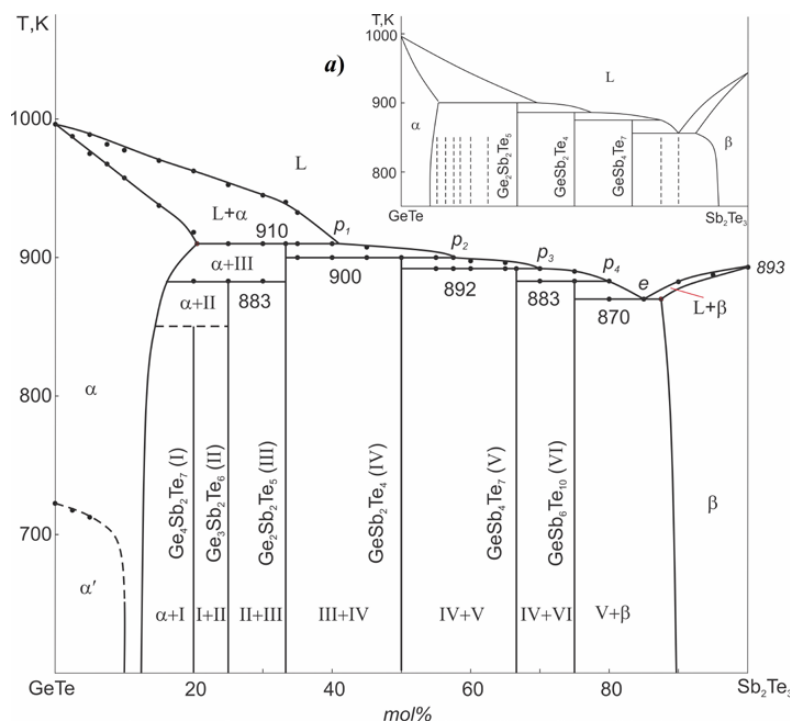


**Fig. 1.** Phase diagram of the GeTe-Sb<sub>2</sub>Te<sub>3</sub>-Te system [46]. a) Compilation phase diagram according to [44, 45]

and identified by DTA and X-ray diffraction techniques. The synthesis was carried out by melting high-purity elemental components in quartz ampoules evacuated to a residual pressure of  $\sim 10^{-2}$  Pa. At the second stage, intermediate alloys of the GeTe-Sb<sub>2</sub>Te<sub>3</sub>-Te system were obtained by fusing the obtained tellurides, as well as elemental tellurium in various stoichiometric ratios, also under vacuum conditions.

At the second stage of synthesis, the results of works [46–48] were taken into account, which showed that even long-term (up to 3000 h) thermal annealing of bulk samples of layered tetradymite-like phases obtained by the traditional method of alloying does not lead to reaching the equilibrium state. According to the authors of the mentioned works, this is due to weak diffusion between the layers in the layered structure of the phases. Taking into account the results of these works, the alloys after alloying were quenched by throwing them into ice water with subsequent homogenizing annealing. Quenching was carried out in the temperature range of 900–1050 K depending on the composition, and homogenizing annealing was carried out at 620 K for 1000 h. Then the alloys were cooled in the switched-off furnace mode.

## 2.2. Methods

Differential thermal analysis (DTA), X-ray diffraction analysis (XRD), and scanning electron microscopy (SEM) were used for the alloys investigations.

Thermal heating curves were recorded on a differential scanning calorimeter DSC NETZSCH 404 F1 Pegasus system and on a multichannel DTA setup assembled based on an electronic data recorder “TC-08 Thermocouple Data Logger”. Powder diffraction patterns were obtained on a Bruker D8 diffractometer with CuK $\alpha$  radiation, and SEM images were collected on a Tescan Vega 3 SBH scanning electron microscope.

## 3. Results and discussion

Analysis of the set of obtained experimental results of annealed samples along different sections of the GeTe-Sb<sub>2</sub>Te<sub>3</sub>-Te concentration triangle using literature data on the системам GeTe-Te [49, 50], Sb<sub>2</sub>Te<sub>3</sub>-Te [50] and GeTe-Sb<sub>2</sub>Te<sub>3</sub> [46] boundary systems allowed to obtain a mutually consistent picture of phase equilibria in the studied system (Fig. 2–8, Table). In the text, figures and table we have adopted the following designations of phases:  $\alpha$ - and  $\alpha'$ -solid solutions based on high-temperature (HT) and low-temperature (RT) modifications of GeTe,

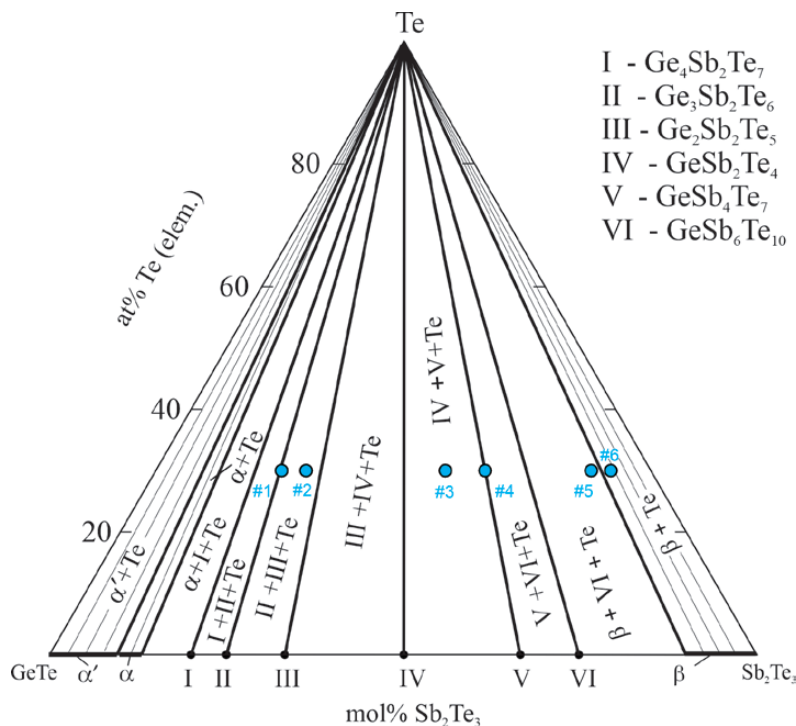


**Fig. 2.** Solid-phase equilibria diagram of the GeTe-Sb<sub>2</sub>Te<sub>3</sub>-Te system at 300 K

$\beta$ -solid solutions based on Sb<sub>2</sub>Te<sub>3</sub>, I-VI – ternary compounds Ge<sub>4</sub>Sb<sub>2</sub>Te<sub>7</sub>, Ge<sub>3</sub>Sb<sub>2</sub>Te<sub>6</sub>, Ge<sub>2</sub>Sb<sub>2</sub>Te<sub>5</sub>, GeSb<sub>2</sub>Te<sub>4</sub>, GeSb<sub>4</sub>Te<sub>7</sub> and GeSb<sub>6</sub>Te<sub>10</sub>, respectively (Fig. 2).

### 3.1. Solid-phase equilibria diagram

Fig. 2 shows an isothermal section of the phase diagram at 300 K. As can be seen, it is characterized by the presence of stable tie-lines between elemental tellurium and all crystalline phases of the GeTe-Sb<sub>2</sub>Te<sub>3</sub> side system. The two-phase regions  $\alpha'$ +Te and  $\beta$ +Te occupy a significant part of the area of the concentration triangle. Other possible two-phase regions are practically degenerated into tie-lines between ternary compounds and elemental tellurium, which is due to the insignificance of their homogeneity regions.

All phase regions in Fig. 2 are confirmed by X-ray diffraction and SEM methods. As can be seen from Fig. 3, the powder diffraction patterns of alloys, which are on the tie-lines in composition, consist of reflection lines of the corresponding ternary compounds and elemental tellurium, and the diffraction patterns of alloys from the Ge<sub>3</sub>Sb<sub>2</sub>Te<sub>6</sub>-Ge<sub>2</sub>Sb<sub>2</sub>Te<sub>5</sub>-Te and GeSb<sub>2</sub>Te<sub>4</sub>-GeSb<sub>4</sub>Te<sub>7</sub>-Te three-phase regions contain diffraction reflections of the corresponding three phases.

The SEM patterns were also in accordance with the solid-phase equilibria diagram. As an example, Fig. 4 shows the SEM patterns of two alloys (samples 5 and 6 in Fig. 2), which clearly show the interface between the  $\beta$ +Te and GeSb<sub>6</sub>Te<sub>10</sub>+ $\beta$ +Te phase regions.

### 3.2. Liquidus surface

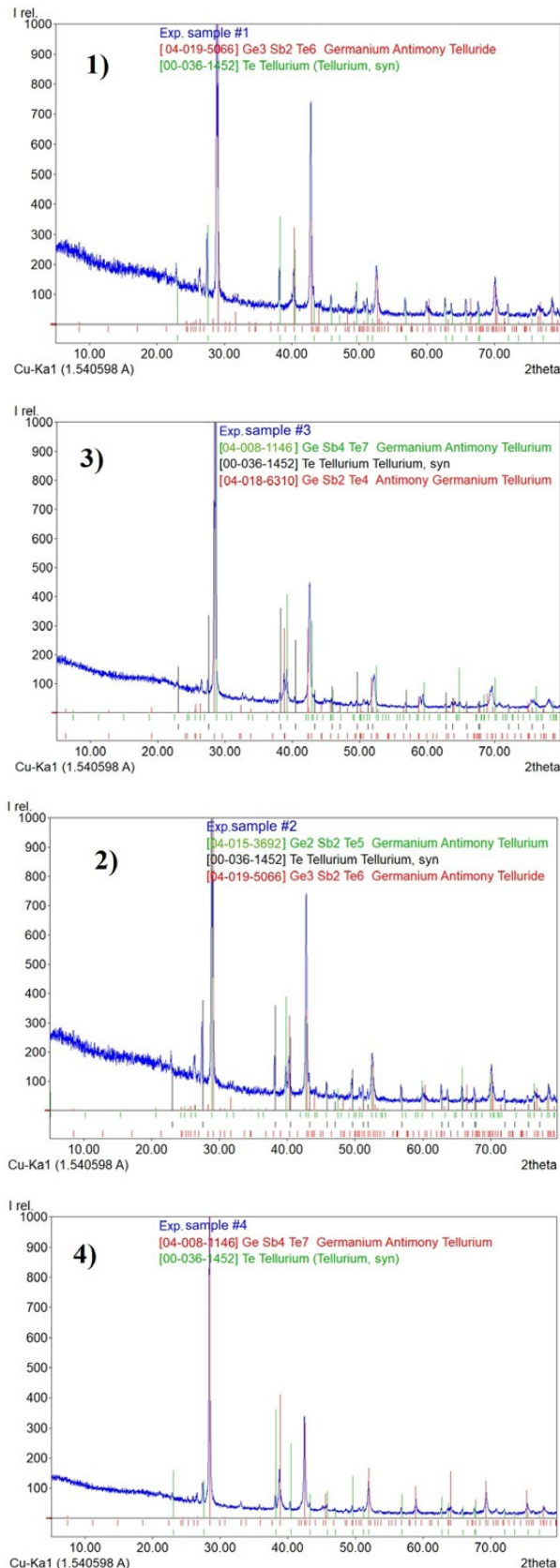
Fig. 5 shows the projection of the liquidus surface of the GeTe-Sb<sub>2</sub>Te<sub>3</sub>-Te system. As can be seen, it consists of the fields of primary crystallization of seven phases:  $\alpha$ - and  $\beta$ -solid solutions, ternary compounds Ge<sub>2</sub>Sb<sub>2</sub>Te<sub>5</sub>, GeSb<sub>2</sub>Te<sub>4</sub>, GeSb<sub>4</sub>Te<sub>7</sub>, GeSb<sub>6</sub>Te<sub>10</sub>, and elemental tellurium. All liquidus surfaces of telluride phases have the form of stripes from the GeTe-Sb<sub>2</sub>Te<sub>3</sub> side system towards the tellurium angle of the concentration triangle.

The primary crystallization fields of phases are delimited by a series of curves of monovariant equilibria, which originate from various points of nonvariant equilibria of the boundary systems. The indicated curves, intersecting near the tellurium angle of the concentration triangle, form a series of points with nonvariant transition (U<sub>1</sub>-U<sub>4</sub>) and eutectic (E) equilibria. The types and temperatures of all non- and monovariant equilibria are given in Table.

**Table.** Non- and monovariant equilibria in the GeTe-Sb<sub>2</sub>Te<sub>3</sub>-Te system

Points and curves in Fig. 5	Equilibrium	T, K
p <sub>1</sub>	L + $\alpha \leftrightarrow \text{Ge}_2\text{Sb}_2\text{Te}_5$	910
p <sub>2</sub>	L + $\text{Ge}_2\text{Sb}_2\text{Te}_5 \leftrightarrow \text{GeSb}_2\text{Te}_4$	900
p <sub>3</sub>	L + $\text{GeSb}_2\text{Te}_4 \leftrightarrow \text{GeSb}_4\text{Te}_7$	892
p <sub>4</sub>	L + $\text{GeSb}_4\text{Te}_7 \leftrightarrow \text{GeSb}_6\text{Te}_{10}$	883
e <sub>1</sub>	$\text{L} \leftrightarrow \text{GeSb}_6\text{Te}_{10} + \beta$	873
e <sub>2</sub>	$\text{L} \leftrightarrow \alpha' + \text{Te}$	653
e <sub>3</sub>	$\text{L} \leftrightarrow \beta + \text{Te}$	695
U <sub>1</sub>	$\text{L} + \beta \leftrightarrow \text{GeSb}_2\text{Te}_4 + \text{Te}$	688
U <sub>2</sub>	$\text{L} + \text{GeSb}_6\text{Te}_{10} \leftrightarrow \text{GeSb}_4\text{Te}_7 + \text{Te}$	677
U <sub>3</sub>	$\text{L} + \text{GeSb}_4\text{Te}_7 \leftrightarrow \text{GeSb}_2\text{Te}_4 + \text{Te}$	665
U <sub>4</sub>	$\text{L} + \text{GeSb}_2\text{Te}_4 \leftrightarrow \text{Ge}_2\text{Sb}_2\text{Te}_5 + \text{Te}$	651
E	$\text{L} \leftrightarrow \alpha' + \text{Ge}_2\text{Sb}_2\text{Te}_5 + \text{Te}$	640
p <sub>1</sub> K <sub>1</sub>	$\text{L} + \alpha_1 \leftrightarrow \text{Ge}_2\text{Sb}_2\text{Te}_5$	910–825
p <sub>2</sub> K <sub>2</sub>	$\text{L} + \text{Ge}_2\text{Sb}_2\text{Te}_5 \leftrightarrow \text{GeSb}_2\text{Te}_4$	900–830
p <sub>3</sub> K <sub>3</sub>	$\text{L} + \text{GeSb}_2\text{Te}_4 \leftrightarrow \text{GeSb}_4\text{Te}_7$	892–840
p <sub>4</sub> K <sub>4</sub>	$\text{L} + \text{GeSb}_4\text{Te}_7 \leftrightarrow \text{GeSb}_6\text{Te}_{10}$	883–850
e <sub>1</sub> K <sub>5</sub>	$\text{L} \leftrightarrow \text{GeSb}_6\text{Te}_{10} + \beta$	873–855
K <sub>5</sub> U <sub>1</sub>	$\text{L} + \beta \leftrightarrow \text{GeSb}_2\text{Te}_4$	855–688
K <sub>4</sub> U <sub>2</sub>	$\text{L} + \text{GeSb}_6\text{Te}_{10} \leftrightarrow \text{GeSb}_4\text{Te}_7$	850–677
K <sub>5</sub> U <sub>3</sub>	$\text{L} + \text{GeSb}_4\text{Te}_7 \leftrightarrow \text{GeSb}_2\text{Te}_4$	840–665
K <sub>2</sub> U <sub>4</sub>	$\text{L} + \text{GeSb}_2\text{Te}_4 \leftrightarrow \text{Ge}_2\text{Sb}_2\text{Te}_5$	830–651
K <sub>1</sub> E	$\text{L} \leftrightarrow \alpha_1(\alpha_2) + \text{Ge}_2\text{Sb}_2\text{Te}_5$	835–640
e <sub>3</sub> U <sub>1</sub>	$\text{L} \leftrightarrow \beta + \text{Te}$	695–688
U <sub>1</sub> U <sub>2</sub>	$\text{L} \leftrightarrow \text{GeSb}_6\text{Te}_{10} + \text{Te}$	688–677
U <sub>2</sub> U <sub>3</sub>	$\text{L} \leftrightarrow \text{GeSb}_4\text{Te}_7 + \text{Te}$	677–665
U <sub>3</sub> U <sub>4</sub>	$\text{L} \leftrightarrow \text{GeSb}_2\text{Te}_4 + \text{Te}$	665–651
U <sub>4</sub> E	$\text{L} \leftrightarrow \text{Ge}_2\text{Sb}_2\text{Te}_5 + \text{Te}$	651–640
e <sub>2</sub> E	$\text{L} \leftrightarrow \alpha_2 + \text{Te}$	653–640

According to Fig. 5, the curves emanating from the peritectic (P<sub>1</sub>-P<sub>4</sub>) and eutectic (e<sub>1</sub>) points of the GeTe-Sb<sub>2</sub>Te<sub>3</sub> boundary system undergo transformations at certain transition points K<sub>1</sub>-K<sub>5</sub>. These transformations can be explained based on phase diagrams of the boundary components of the studied system. Thus, in the side system GeTe-Sb<sub>2</sub>Te<sub>3</sub>, the temperatures of the peritectic (P<sub>1</sub>-P<sub>4</sub>) and eutectic (e<sub>1</sub>) equilibria decrease in the direction from germanium telluride to Sb<sub>2</sub>Te<sub>3</sub>, i.e. from left to right in Fig. 5. At the same time, in the side system GeTe-Te, the temperature of the eutectic e<sub>2</sub> (653 K) is significantly lower than that of the eutectic e<sub>3</sub> (695 K) in the other boundary system Sb<sub>2</sub>Te<sub>3</sub>-Te, i.e. in this part of the phase diagram, the temperatures of the invariant equilibria decrease in the opposite direction. The

**Fig. 3.** Powder diffraction patterns of alloys 1-4, shown in Fig. 2

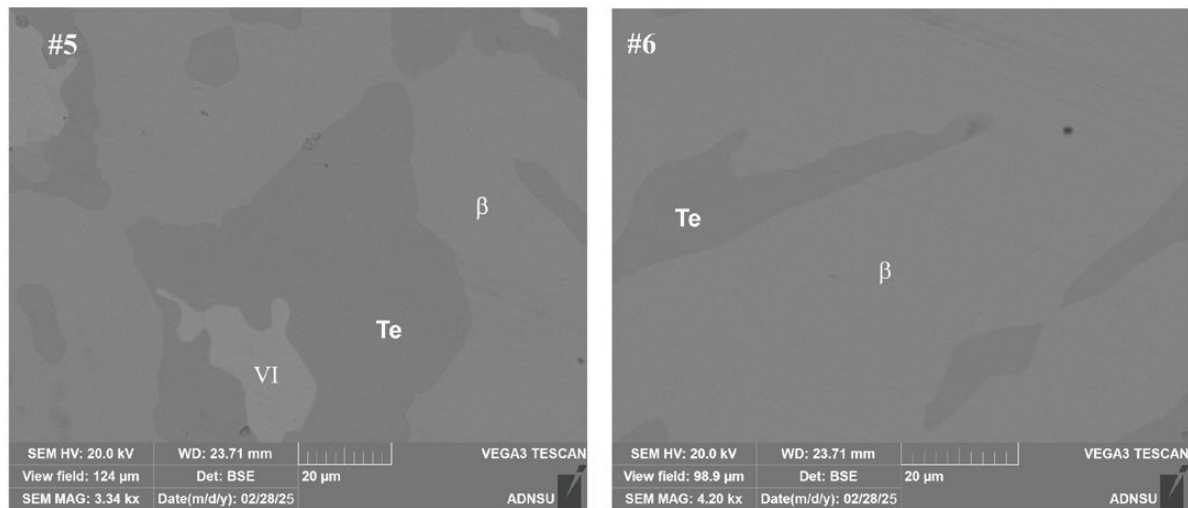


Fig. 4. SEM patterns of alloys 5 and 6, shown in Fig. 2

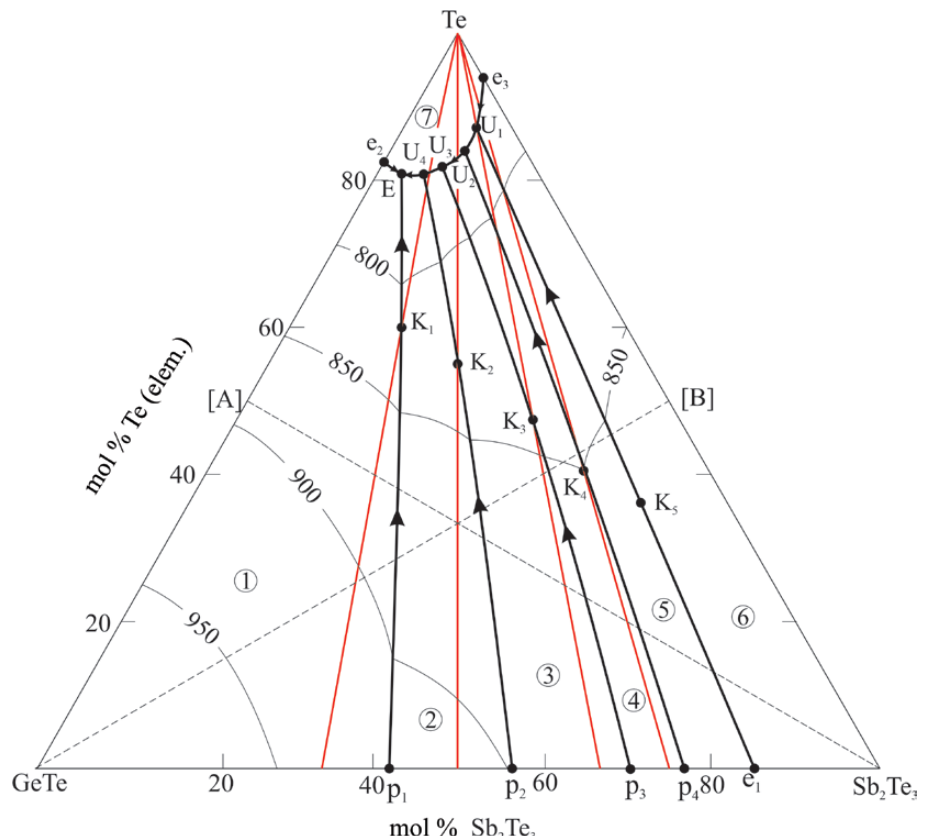


Fig. 5. Projection of the liquidus surface of the GeTe-Sb<sub>2</sub>Te<sub>3</sub>-Te system. Primary crystallization fields: 1 –  $\alpha$ ; 2 – Ge<sub>2</sub>Sb<sub>2</sub>Te<sub>5</sub>; 3 – GeSb<sub>2</sub>Te<sub>4</sub>; 4 – GeSb<sub>4</sub>Te<sub>7</sub>; 5 – GeSb<sub>6</sub>Te<sub>10</sub>; 6 –  $\beta$ ; 7 – Te

experimental DTA data obtained by us showed that the temperatures of nonvariant transition equilibria (U<sub>1</sub>-U<sub>4</sub>) also decrease in the direction from the eutectic e<sub>3</sub> to the ternary eutectic point E (640 K) (Fig. 5, Table). Similar opposite directions of changes in the temperatures of nonvariant equilibria in the boundary system GeTe- Sb<sub>2</sub>Te<sub>3</sub> and in the regions of compositions

rich in tellurium lead to the transformation of the above-mentioned monovariant equilibria [51, 52]. In the case of peritectic equilibrium curves, similar transformations occur at the intersection points (K<sub>1</sub>-K<sub>4</sub>) of the pointed curves with the corresponding stable sections of the “ternary compound-elementary tellurium” type (Fig. 5). Therefore, in the Table, the pointed curves are

presented as two series, transforming into each other at the transition points K<sub>1</sub>-K<sub>5</sub> (Fig. 5).

Using the curve P<sub>1</sub>E as an example, we will consider one of the above transformations. This curve, before intersecting with the stable section Ge<sub>2</sub>Sb<sub>2</sub>Te<sub>5</sub>-Te (P<sub>1</sub>K<sub>1</sub>), reflects the peritectic equilibrium L + α ↔ III. At the intersection point (K<sub>1</sub>), this equilibrium is transformed into the eutectic L ↔ α + III (curve K<sub>1</sub>E). Similar transformations take place on the P<sub>2</sub>U<sub>4</sub>, P<sub>3</sub>U<sub>3</sub>, P<sub>4</sub>U<sub>2</sub> and e<sub>1</sub>U<sub>1</sub> curves.

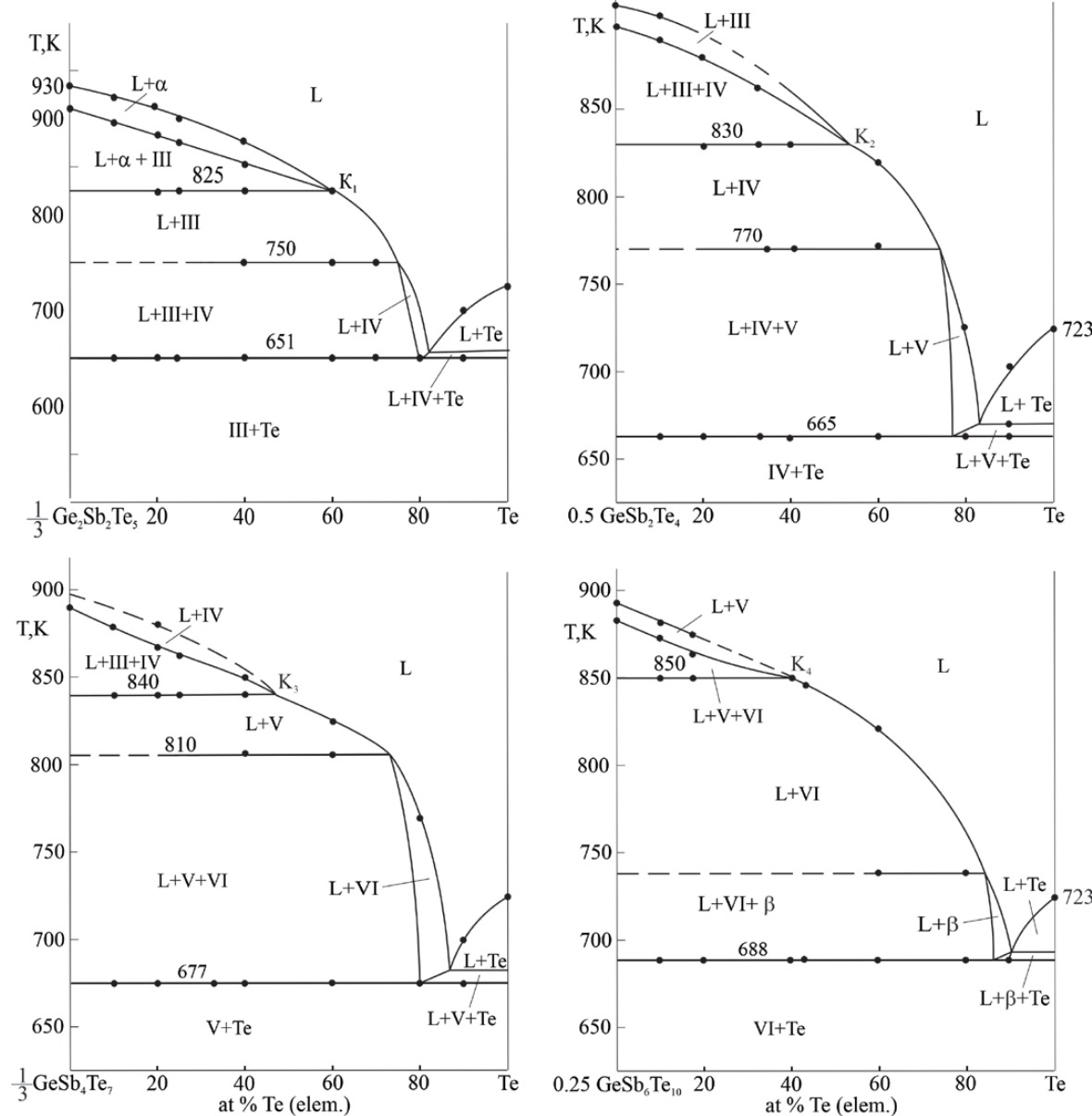


**Fig. 6.** Polythermal sections of Ge<sub>2</sub>Sb<sub>2</sub>Te<sub>5</sub>-Te, GeSb<sub>2</sub>Te<sub>4</sub>-Te, GeSb<sub>4</sub>Te<sub>7</sub>-Te и GeSb<sub>6</sub>Te<sub>10</sub>-Te of the phase diagram of the GeTe-Sb<sub>2</sub>Te<sub>3</sub>-Te system

### 3.3. Polythermal sections of the phase diagram

Below some polythermal sections of the T-x-y phase diagram of the GeTe-Sb<sub>2</sub>Te<sub>3</sub>-Te system (Fig. 6–8) are presented, which reflect the crystallization processes in more detail and made it possible to clarify the location of the curves of monovariant equilibria and the coordinates of the invariant points.

Four (Ge<sub>2</sub>Sb<sub>2</sub>Te<sub>5</sub>-Te, GeSb<sub>2</sub>Te<sub>4</sub>-Te, GeSb<sub>4</sub>Te<sub>7</sub>-Te and GeSb<sub>6</sub>Te<sub>10</sub>-Te) of the six polythermal sections considered are stable in the subsolidus. Two other

sections GeTe-[B] and [A]-Sb<sub>2</sub>Te<sub>3</sub> ([A] and [B] are alloys with equimolar ratios of components of the boundary systems GeTe-Te and Sb<sub>2</sub>Te<sub>3</sub>-Te, respectively) intersect almost all fields of primary crystallization of phases and reflect most heterogeneous equilibria.

**Ge<sub>2</sub>Sb<sub>2</sub>Te<sub>5</sub>-Te section** (Fig. 6) passes through the fields of primary crystallization of the  $\alpha$ -phase, Ge<sub>2</sub>Sb<sub>2</sub>Te<sub>5</sub> and GeSb<sub>2</sub>Te<sub>4</sub> compounds as well as elemental tellurium. Below the  $\alpha$ -phase liquidus, crystallization proceeds according to the  $L + \alpha \leftrightarrow Ge_2Sb_2Te_5$  peritectic reaction (Fig. 5, curve P<sub>K1</sub>), resulting in the formation of a three-phase field L +  $\alpha$  + Ge<sub>2</sub>Sb<sub>2</sub>Te<sub>5</sub>. In this reaction, the  $\alpha$ -phase is completely consumed and at 825 K the system passes into a two-phase state L + Ge<sub>2</sub>Sb<sub>2</sub>Te<sub>5</sub>. Starting from 750 K, crystallization continues according to the peritectic reaction  $L + GeSb_2Te_4 \leftrightarrow Ge_2Sb_2Te_5$  (Fig. 5, curve K<sub>2</sub>U<sub>4</sub>), as a result of which a three-phase region L + Ge<sub>2</sub>Sb<sub>2</sub>Te<sub>5</sub> + GeSb<sub>2</sub>Te<sub>4</sub> is formed.

Near the tellurium angle, tellurium crystallizes primarily from the melt, then the monovariant

eutectic process  $L \leftrightarrow GeSb_2Te_4 + Te$  begins (Fig. 5, curve U<sub>3</sub>U<sub>4</sub>). Complete crystallization of the alloys of this section occurs at 651 K according to the invariant transition reaction U<sub>4</sub> and a two-phase mixture GeSb<sub>2</sub>Te<sub>4</sub> + Te is formed. The crystallization processes along the other three sections connecting the compositions of ternary compounds with elemental tellurium (Fig. 6) can be followed by comparing them with Figs. 2 and 5. As can be seen from the T-diagrams, despite the stability of these sections below the solidus, the crystallization processes in them are complex and multi-stage.

**The GeTe-[B] section** (Fig. 7) passes through the fields of primary crystallization of all phases except elemental tellurium (Fig. 5). In the subsolidus it crosses all phase regions of the system (Fig. 2). In this diagram, the liquidus curves of different phases are marked taking into account Fig. 5. Pairs of conjugate curves emanating from the intersection points of the liquidus lines reflect the beginning and the

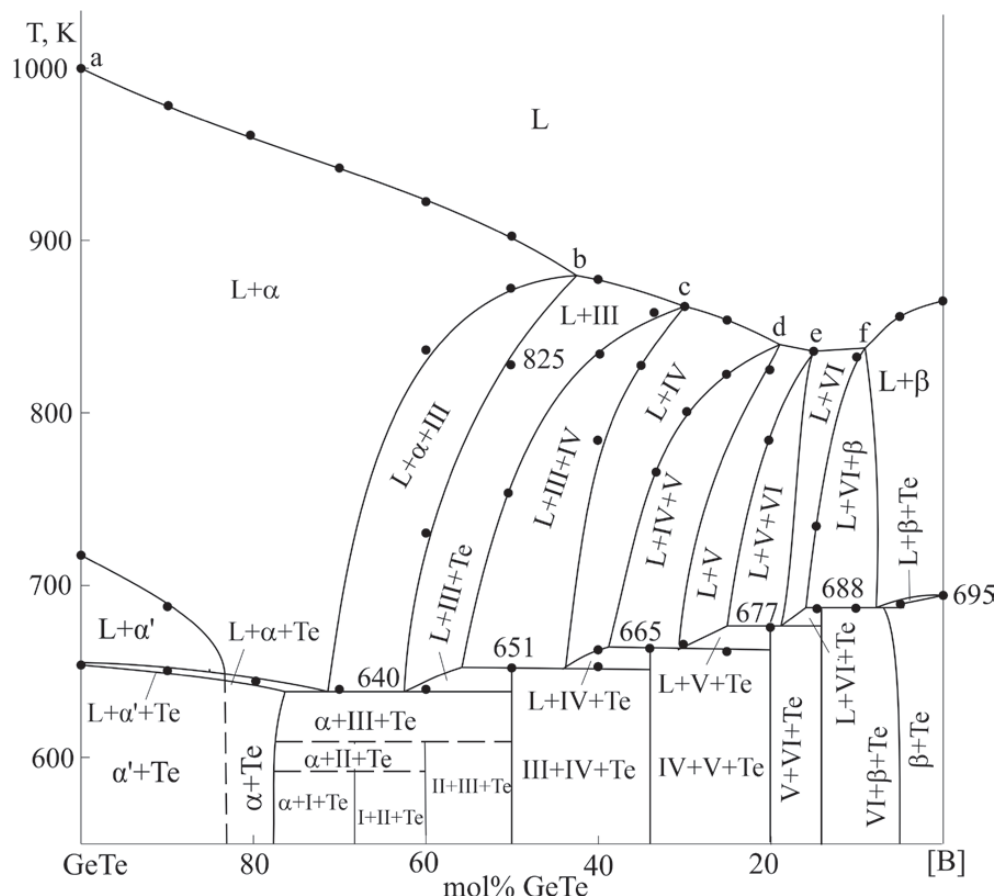
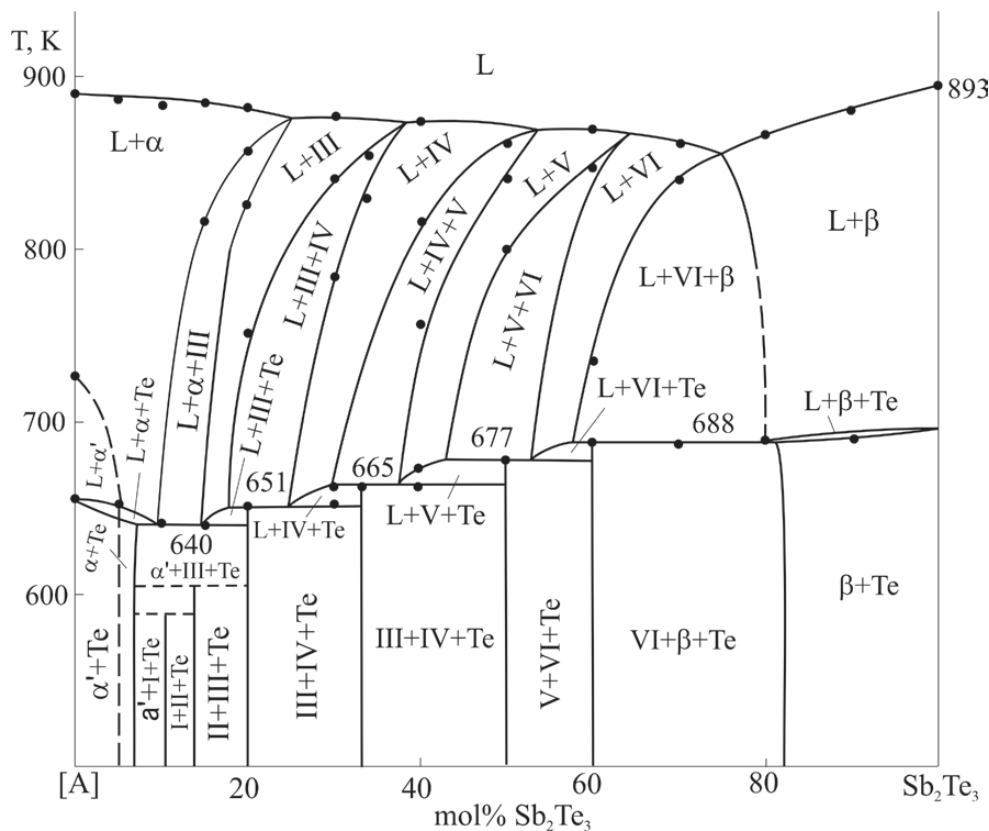


Fig. 7. Polythermal section of GeTe-[B] of the phase diagram of the GeTe-Sb<sub>2</sub>Te<sub>3</sub>-Te system



**Fig. 8.** Polythermal section of [A]-Sb<sub>2</sub>Te<sub>3</sub> of the phase diagram of the GeTe-Sb<sub>2</sub>Te<sub>3</sub>-Te system

end of monovariant equilibria along the curves P<sub>1</sub>K<sub>1</sub>E (b), P<sub>2</sub>K<sub>2</sub>U<sub>4</sub> (c), P<sub>3</sub>K<sub>3</sub>U<sub>3</sub> (d), P<sub>4</sub>K<sub>4</sub>U<sub>2</sub> (e), P<sub>1</sub>K<sub>5</sub>U<sub>1</sub> (f). The fields between the indicated pairs of curves correspond to the two-phase areas L+III (IV, V, VI) and L + β. These pairs of curves in the temperature range of 640–688 K reach the curves of monovariant equilibria originating from the eutectic points e<sub>2</sub> and e<sub>3</sub> of the side systems and form a series of transition points (U<sub>1</sub>, U<sub>2</sub>, U<sub>3</sub>, U<sub>4</sub>) and eutectic (E) equilibria (Fig. 5). The horizontals at 688, 677, 665, 651 and 640 K in Fig. 7 reflect these nonvariant equilibria.

**Section [A]-Sb<sub>2</sub>Te<sub>3</sub>** (Fig. 8). Phase equilibria along this section are qualitatively similar to those in Fig. 7 and differ from them only in temperature-concentration intervals.

#### 4. Conclusion

Based on the experimental data obtained by studying carefully homogenized equilibrium alloys using the DTA, XRD and SEM methods, a new refined picture of phase equilibria in the GeTe-Sb<sub>2</sub>Te<sub>3</sub>-Te system was obtained, which significantly differs from the previously known

one. A solid-phase equilibria diagram at 300 K and a projection of the liquidus surface, as well as a number of polythermal sections of the phase diagram, were constructed. The fields of primary crystallization of seven phases, including ternary compounds Ge<sub>2</sub>Sb<sub>2</sub>Te<sub>5</sub>, GeSb<sub>2</sub>Te<sub>4</sub>, GeSb<sub>4</sub>Te<sub>7</sub> and GeSb<sub>6</sub>Te<sub>10</sub> were determined, non- and monovariant equilibria were established. It was shown that monovariant equilibria on the curves of monovariant equilibria undergo transformations at certain transition points. The interaction of the indicated curves with the eutectic curves emanating from the lateral systems GeTe-Te and Sb<sub>2</sub>Te<sub>3</sub>-Te leads to a cascade of invariant transition reactions characterizing the joint crystallization of two-phase mixtures III(IV, V, VI)+Te.

The results obtained in the work can be used to obtain poly- and single crystals of the above-mentioned ternary compounds, which are promising as topological insulators, thermoelectrics and materials with phase memory.

## Contribution of the authors

The authors contributed equally to this article.

## Conflict of interests

The authors declare that they have no known competing financial interests or personal relationships that could have influenced the work reported in this paper.

## References

- Shevelkov A. V. Chemical aspects of the design of thermoelectric materials. *Russian Chemical Reviews*. 2008;77: 1–19. <https://doi.org/10.1070/rc2008v077n01abeh003746>
- Sootsman J. R., Chung D. Y., Kanatzidis M. G. New and old concepts in thermoelectric materials. *Angewandte Chemie International Edition*. 2009;48: 8616–8639. <https://doi.org/10.1002/anie.200900598>
- Ma W., Record M., Tian J., Boulet P. Strain effects on the electronic and thermoelectric properties of n(PbTe)-m(Sb<sub>2</sub>Te<sub>3</sub>) system compounds. *Materials*. 2021;14(15): 4086–4095. <https://doi.org/10.3390/ma14154086>
- Xu B., Feng T., Li Z., Zhou L., Pantelides S. T., Wu Y. Creating zipper-like van Der Waals gap discontinuity in low-temperature-processed nanostructured PbSb<sub>2n</sub>Te<sub>1+3n</sub>: enhanced phonon scattering and improved thermoelectric performance. *Angewandte Chemie International Edition*. 2018;57: 10938–10943. <https://doi.org/10.1002/anie.201805890>
- Xiao Y., Xianli S., Yonggao Y., Xinfeng T. Structures and thermoelectric properties of (GeTe)<sub>n</sub>Bi<sub>2</sub>Te<sub>3</sub>. *Journal of Inorganic Materials*. 2021;36(1): 75–80. <https://doi.org/10.15541/jim20200252>
- Kihoi S. K., Shenoy U. S., Kahiu J. N., Kim H., Bhat D. K., Lee H. S. Tailoring the thermoelectric performance of the layered topological insulator SnSb<sub>2</sub>Te<sub>4</sub> through Sb positional doping at the Sn and Sb cation sites. *ACS Applied Electronic Materials*. 2023;5(8): 4504–4513. <https://doi.org/10.1021/acsaelm.3c00685>
- Kane C. L., Moore J. E. Topological insulators. *Physics World*. 2011;24(2): 32–36. <https://doi.org/10.1088/2058-7058/24/02/36>
- Moore J. E., The birth of topological insulator. *Nature*. 2010;464: 194–198. <https://doi.org/10.1038/nature08916>
- Heremans J. P., Cava R. J., Samarth N. Tetradymites as thermoelectrics and topological insulators. *Nature Reviews Materials*. 2017;2: 17049. <https://doi.org/10.1038/natrevmats.2017.49>
- Politano A., Caputo M., Nappini S., ... Chulkov E. Exploring the surface chemical reactivity of single crystals of binary and ternary bismuth chalcogenides. *Journal of Physical Chemistry C*. 2014;118: 21517–21522. <https://doi.org/10.1021/jp506444f>
- Shvets I. A., Klimovskikh I. I., Aliev Z. S., ... Chulkov E. V. Impact of stoichiometry and disorder on the electronic structure of the PbSb<sub>2</sub>Te<sub>4-x</sub>Se<sub>x</sub> topological insulator. *Physical Review B*. 2017;96: 235124–235127. <https://doi.org/10.1103/physrevb.96.235124>
- Pacilè D., Eremeev S. V., Caputo M., ... Papagno M. Deep insight into the electronic structure of ternary topological insulators: a comparative study of PbBi<sub>4</sub>Te<sub>7</sub> and PbBi<sub>6</sub>Te<sub>10</sub>. *Physica Status Solidi. Rapid Research Letters*. 2018; 1800341–1800348. <https://doi.org/10.1002/pssr.201800341>
- Shvets I. A., Klimovskikh I. I., Aliev Z. S., ... Chulkov E. V. Surface electronic structure of the wide band gap topological insulator PbBi<sub>4</sub>Te<sub>4</sub>Se<sub>3</sub>. *Physical Review B*. 2019;100(19): 195127. <https://doi.org/10.1103/PhysRevB.100.195127>
- Jahangirli Z. A., Alizade E. H., Aliev Z. S., ... Chulkov E. V. Electronic structure and dielectric function of Mn-Bi-Te layered compounds. *Journal of Vacuum Science & Technology B, Nanotechnology and Microelectronics: Materials, Processing, Measurement, and Phenomena*. 2019;37: 062910. <https://doi.org/10.1116/1.5122702>
- Wu Z., Liang G., Pang W. ... Guo Z. Coupling topological insulator SnSb<sub>2</sub>Te<sub>4</sub> nanodots with highly doped graphene for high-rate energy storage. *Advanced Material*. 2019;32(2): 1905632. <https://doi.org/10.1002/adma.201905632>
- Klimovskikh I., Otrokov M. M., Estyunin D. Tunable 3D/2D magnetism in the (MnBi<sub>2</sub>Te<sub>4</sub>)(Bi<sub>2</sub>Te<sub>3</sub>)<sub>m</sub> topological insulators family. *npj Quantum Mater*. 2020;5: 54. <https://doi.org/10.1038/s41535-020-00255-9>
- Hattori Y., Tokumoto Y., Kimoto K. Evidences of inner Se ordering in topological insulator PbBi<sub>2</sub>Te<sub>4</sub>-PbBi<sub>2</sub>Se<sub>4</sub>-PbSb<sub>2</sub>Se<sub>4</sub> solid solutions. *Science Reports*. 2020;10: 7957. <https://doi.org/10.1038/s41598-020-64742-6>
- Tominaga J. Topological memory using phase-change materials. *MRS Bulletin*. 2018;43(5): 347–351. <https://doi.org/10.1557/mrs.2018.94>
- Jones R. O. Phase change memory materials: rationalizing the dominance of Ge/Sb/Te alloys. *Physical Review B*. 2020;101(2): 024103. <https://doi.org/10.1103/PhysRevB.101.024103>
- Cao T., Wang R., Simpson R. E., Li G. Photonic Ge-Sb-Te phase change metamaterials and their applications. *Progress in Quantum Electronics*. 2020;74: 100299. <https://doi.org/10.1016/j.pquantelec.2020.100299>
- Wang D., Zhao L., Yu S., ... Zhang W. Non-volatile tunable optics by design: from chalcogenide phase-change materials to device structures. *Materials Today*. 2023;68: 334–355. <https://doi.org/10.1016/j.mattod.2023.08.001>
- Sun C. W., Youm M. S., Kim Y. T. Crystallization behavior of non-stoichiometric Ge-Bi-Te ternary phase change materials for PRAM application. *Journal of Physics: Condensed Matter*. 2007;19: 446004. <https://doi.org/10.1088/0953-8984/19/44/446004>
- Cui Y., Zhang Y., Cheng Z. Nonvolatile displays based on phase change materials. *Advanced Optical Materials*. 2023;11(21): 2300481. <https://doi.org/10.1002/adom.202300481>
- Gavdush A. A., Komandin G. A., Bukin V. V., ... Shi Q. Terahertz-infrared spectroscopy of Ge<sub>2</sub>Sb<sub>2</sub>Te<sub>5</sub> films on sapphire: evolution of broadband electrodynamic response upon phase transitions. *Journal of Applied Physics*. 2023;134: 085103. <https://doi.org/10.1063/5.0160772>
- West D. R. F. *Ternary phase diagrams in materials science*. 3rd edn. London: CRC Press; 2020. 240 p. <https://doi.org/10.1201/9781003077213>
- Babanly M. B., Chulkov E. V., Aliev Z. S., Shevel'kov A. V., Amiraslanov I. R. Phase diagrams in materials science of topological insulators based on metal

chalkogenides. *Russian Journal of Inorganic Chemistry*. 2017;62(13): 1703–1729. <https://doi.org/10.1134/S0036023617130034>

27. Babanly M. B., Yusibov Y. A., Imamaliyeva S. Z., Babanly D. M., Alverdiyev I. J. Phase diagrams in the development of the argyrodite family compounds and solid solutions based on them. *Phase Equilibria and Diffusion*. 2024;45: 228–255. <https://doi.org/10.1007/s11669-024-01088-w>

28. Babanly M. B., Mashadieva L. F., Imamalieva S. Z., Babanly D. M., Tagiev D. B., Yusibov Yu. A. Complex copper-based chalcogenides: a review of phase equilibria and thermodynamic properties. *Condensed Matter and Interphases*. 2024;26(4): 579–619. <https://doi.org/10.17308/kcmf.2024.26/12367>

29. Cantor B. Exploring multicomponent phase space to discover new materials. *Journal Phase Equilibria and Diffusion*. 2024;45: 188–218. <https://doi.org/10.1007/s11669-024-01131-w>

30. Seidzade A. E., Orujlu E. N., Doert T., Babanly M. B. An updated phase diagram of the SnTe-Sb<sub>2</sub>Te<sub>3</sub> system and the crystal structure of the new compound SnSb<sub>4</sub>Te<sub>7</sub>. *Journal Phase Equilibria and Diffusion*. 2021;42: 373–378. <https://doi.org/10.1007/s11669-021-00888-8>

31. Gojayeva I. M., Babanly V. I., Aghazade A. I., Orujlu E. N. Experimental reinvestigation of the PbTe–Sb<sub>2</sub>Te<sub>3</sub> pseudo-binary system. *Azerbaijan Chemical Journal*. 2022;2: 47–53. <https://doi.org/10.32737/0005-2531-2022-2-47-53>

32. Orujlu E. N., Seidzade A. E., Babanly D. M., Amiraslanov I. R., Babanly M. B. New insights into phase equilibria of the SnTe–Sb<sub>2</sub>Te<sub>3</sub> pseudo-binary system: synthesis and crystal structure of new tetradyomite-type compound Sn<sub>3</sub>Sb<sub>2</sub>Te<sub>6</sub>. *Journal of Solid State Chemistry*. 2024;330: 124494. <https://doi.org/10.1016/j.jssc.2023.124494>

33. Alakbarova T. M., Meyer H.-J., Orujlu E. N., Amiraslanov I. R., Babanly M. B. Phase equilibria of the GeTe–Sb<sub>2</sub>Te<sub>3</sub> quasi-binary system in the range 0–50 mol % Sb<sub>2</sub>Te<sub>3</sub>. *Phase Transitions*. 2021;94(5): 366–375. <https://doi.org/10.1080/01411594.2021.1937625>

34. Alakbarova T. M. Meyer H.-J., Orujlu E. N. A refined phase diagram of the GeTe–Sb<sub>2</sub>Te<sub>3</sub> system. *Condensed Matter and Interphases*. 2022;24(1): 11–18. <https://doi.org/10.17308/kcmf.2022.24/9050>

35. Alakbarova T. M., Orujlu E. N., Babanly D. M. Solid-phase equilibria in the GeSb<sub>2</sub>Te<sub>4</sub>–Sb<sub>2</sub>Te<sub>3</sub>–Te system and thermodynamic properties of compounds of the GeTe–mSb<sub>2</sub>Te<sub>3</sub> homologous series. *Physics and Chemistry of Solid State*. 2022;23(1): 25–33. <https://doi.org/10.15330/pcss.23.1.25-33>

36. Orujlu E. N., Babanly D. M., Alakbarova T. M., Orujov N. I., Babanly M. B. Study of the solid-phase equilibria in the GeTe–Sb<sub>2</sub>Te<sub>3</sub>–Te system and thermodynamic properties of GeTe-rich germanium bismuth tellurides. *The Journal of Chemical Thermodynamics*. 2024;196: 107323. <https://doi.org/10.1016/j.jct.2024.107323>

37. Orujlu E. N., Alakbarova T. M., Babanly M. B. The GeTe–Bi<sub>2</sub>Te<sub>3</sub>–Te system. *Russian Journal of Inorganic Chemistry*. 2024;68(8): 1144–1154. <https://doi.org/10.31857/S0044457X24080079>

38. Abrikosov N. X., Danilova-Dobryakova G. T. Study of the GeTe–Sb<sub>2</sub>Te<sub>3</sub> phase diagram\*. *Izvestiya Akademii Nauk SSSR, Neorganicheskie Materialy*. 1965;2: 204–207. (in Russ.)

39. Legendre B., Hancheng C., Bordas S., Clavaguera-Mora M. T. Phase diagram of the ternary system Ge–Sb–Te.

I. The subternary GeTe–Sb<sub>2</sub>Te<sub>3</sub>–Te. *Thermochimica Acta*. 1984;78: 141–157. [https://doi.org/10.1016/0040-6031\(84\)87142-7](https://doi.org/10.1016/0040-6031(84)87142-7)

40. Abrikosov N. Kh., Danilova-Dobryakova G. T. System Ge–Sb–Te\*. *Izvestiya Akademii Nauk SSSR, Neorganicheskie Materialy*. 1970; 6(3): 475–481. (in Russ.)

41. Bordas S., Clavaguera-Mora M. T. Legendre B., Hancheng C. Phase diagram of the ternary system Ge–Sb–Te. II. The subternary Ge–GeTe–Sb<sub>2</sub>Te<sub>3</sub>–Sb. *Thermochimica Acta*. 1986;107: 239–265. [https://doi.org/10.1016/0040-6031\(86\)85051-1](https://doi.org/10.1016/0040-6031(86)85051-1)

42. Skoropanov A. S., Valevsky B. L., Skums V. F., Samal G. I., Vecher A. A. Physico-chemical study of Ge(Pb)–Sb<sub>2</sub>(Sb<sub>2</sub>)Te<sub>3</sub> system ternary compounds. *Thermochimica Acta*. 1985;90: 331–334. [https://doi.org/10.1016/0040-6031\(85\)87110-0](https://doi.org/10.1016/0040-6031(85)87110-0)

43. Shelimova L. E., Tomashik V. N., Grytsiv V. I. *State diagrams in semiconductor materials science: systems based on Si, Ge, Sn, Pb\**. Moscow: Nauka Publ.; 1991. 368 p. (in Russ.)

44. Shelimova L. E., Karpinsku O. G., Zemskov V. S., Konstantinov P. P. Structural and electrical properties of layered tetradyomite-like compounds in the GeTe–Bi<sub>2</sub>Te<sub>3</sub> and GeTe–Sb<sub>2</sub>Te<sub>3</sub> systems. *Inorganic Materials*. 2000;36(3): 235–242. <https://doi.org/10.1007/BF02757928>

45. Shelimova L. E., Karpinskii O. G., Konstantinov P. P., Avilov, E. S., Kretova M. A., Zemskov V. S. Crystal structures and thermoelectric properties of layered Compounds in the ATe–Bi<sub>2</sub>Te<sub>3</sub> (A = Ge, Sn, Pb) Systems. *Inorganic Materials*. 2004;40: 451–460. <https://doi.org/10.1023/B:INMA.0000027590.43038.a8>

46. Orujlu E. N., Izzatli S. B., Jafarov Y. I., Babanly M. B. Reinvestigation of the GeTe–Sb<sub>2</sub>Te<sub>3</sub> pseudobinary phase diagram. *Azerbaijan Chemical Journal*. 2025;2: 95–103. <https://doi.org/10.32737/0005-2531-2025-2-95-103>

47. Hasanova G. S., Aghazade A. I., Imamaliyeva S. Z., Yusibov Y. A., Babanly M. B. Refinement of the phase diagram of the Bi–Te system and the thermodynamic properties of lower bismuth tellurides. *JOM*. 2021;73(5): 1511–1521. <https://doi.org/10.1007/s11837-021-04621-1>

48. Hasanova G. S., Aghazade A. I., Babanly D. M., Imamaliyeva S. Z., Yusibov Y. A., Babanly M. B. Experimental study of the phase relations and thermodynamic properties of Bi–Se system. *Journal of Thermal Analysis Calorimetry*. 2021;147: 6403–6414. <https://doi.org/10.1007/s10973-021-10975-0>

49. Bletskan D. I. Phase equilibrium in the systems AIV–BVI. *Journal of Ovonic Research*. 2005;1(5): 53–60. Режим доступа: <https://www.chalcogen.ro/Bletskan1.pdf>

50. *Binary alloy phase diagrams*. T. B. Massalski (ed.). second edition. ASM International. Ohio: Materials Park; 1990. 3589 p.

51. Lutsyk V. I., Vorob'eva V. P., Shodorova S. Ya. Determining the conditions for changes of the three-phase reaction type in a V–Zr–Cr system. *Russian Journal Physical Chemistry A*. 2015;89: 2331. <https://doi.org/10.1134/S0036024415130245>

52. Lutsyk V. I., Vorob'eva V. P. 3D computer models of T–x–y diagrams, forming the Fe–Ni–Co–FeS–NiS–CoS subsystem. *Russian Journal Physical Chemistry A*. 2017;91(13): 2593–2599. <https://doi.org/10.1134/S0036024417130131>

\* Translated by author of the article

## Information about the authors

*Elnur R. Nabihev*, PhD student, Ganja State University (Ganja, Azerbaijan).

<https://orcid.org/0009-0006-1907-3957>

azechemist@gmail.com

*Elnur N. Orujlu*, PhD in Chemistry, Head of “Nanomaterials and Nanotechnologies” Science-Research Laboratory, Azerbaijan State Oil and Industry University (Baku, Azerbaijan).

<https://orcid.org/0000-0001-8955-7910>

elnur.oruclu@yahoo.com

*Alekper A. Hasanov*, Dr. Sci. (Tech.), Professor, Azerbaijan State Oil and Industry University (Baku, Azerbaijan).

elekber.hasanov@asoiu.edu.az

*Aytan I. Aghazade*, PhD student, Researcher at the Institute of Catalysis and Inorganic Chemistry (Baku, Azerbaijan).

<https://orcid.org/0000-0002-6072-1075>

aytenagazade94@gmail.com

*Sevda H. Aliyeva*, PhD student, Nakhchivan State University (Nakhchivan, Azerbaijan).

<https://orcid.org/0009-0007-7737-0578>

sevdaeliyeva@gdu.edu.az

*Yusif A. Yusibov*, Dr. Sci. (Chem.), Professor, Rector of the Ganja State University (Ganja, Azerbaijan).

<https://orcid.org/0000-0003-4081-6170>

yusifyusibov1951@gmail.com

*Received May 29, 2025; approved after reviewing June 16, 2025; accepted for publication July 15, 2025; published online December 25, 2025.*